Upper critical fields of periodic and quasiperiodic Nb-Ta superlattices

J. L. Cohn, J. J. Lin,* F. J. Lamelas, H. He, R. Clarke, and C. Uher
Department of Physics, The University of Michigan, Ann Arbor, Michigan 48109
(Received 23 December 1987; revised manuscript received 11 April 1988)

Upper critical fields have been studied for two series of Nb-Ta superlattices grown by molecular-beam epitaxy with both periodic and quasiperiodic (Fibonacci sequence) layering. X-ray results are presented to characterize the nature and quality of the layering. Positive curvature in the perpendicular upper critical field ($H_{c2\perp}$), pronounced negative curvature near T_c in the parallel upper critical field ($H_{c2\parallel}$), and dimensional crossover are observed in both types of samples. For quasiperiodic samples two upturns are observed in $H_{c2\parallel}$ with decreasing temperature. These are shown to be associated with dimensional crossover occurring twice as the superconducting coherence length in the growth direction, $\xi_\perp$, samples the two length scales, $2d_{\mathrm{Nb}}$ and d_{Nb}, that are present in these structures.

I. INTRODUCTION

Recent theoretical[1-4] and experimental[5-15] efforts in the study of artificially prepared multilayered superconductors have focused on $\cdots S\text{-}N\text{-}S\text{-}N \cdots$ systems where S and N denote superconducting and normal-metal or lower-T_c superconducting layers, respectively. This class of superconducting materials is of intrinsic interest due to the presence of strong proximity coupling between superconducting layers. The Nb-Ta system[5-10] is of particular interest because the close lattice match of the constituents provides for single-crystalline growth, and thus these structures represent a close approximation to perfect metallic superlattices.

Modern deposition techniques such as molecular-beam epitaxy enable the tailoring of materials on a near-atomic scale, and consequently the study of artificially layered materials has become a vast field of research. In addition to a large and growing body of experimental work on periodically modulated structures,[15] several recent studies have addressed quasiperiodic[14,16] and fractal[17] multilayering. Much of the current interest in such systems is the belief that the character of electronic wave functions in a one-dimensional quasiperiodic system interpolates between the extended and localized states characteristic of periodic and random systems, respectively. In this regard, the high quality of the interfaces in Nb-Ta multilayers make this system well suited to a study of the effects of aperiodicity on transport properties. As far as superconductivity is concerned, there is a potentially rich structure in the parallel upper critical field, $H_{c2\parallel}$. Measurements of $H_{c2\parallel}$ provide a direct probe of the interplay between the superconducting coherence length in the growth direction, $\xi_\perp$, and the scale(s) associated with the artificially imposed superlattice modulation. Anomalous behaviors observed in periodic $\cdots S\text{-}N\text{-}S\text{-}N \cdots$ multilayers include dimensional crossover[12] and effects associated with the commensurability of the vortex flux structure[13] with an underlying period in the superlattice.

In this paper we report measurements of parallel and perpendicular upper critical fields in two series of Nb-Ta superlattices with both periodic and quasiperiodic layering. Dimensional crossover occurs in both types of samples and the criterion $\xi_\perp \leq \Lambda = d_{\mathrm{Nb}} + d_{\mathrm{Ta}}$ successfully predicts the dimensional effects. The presence of two Nb length scales in the quasiperiodic samples results in two upturns in $H_{c2\parallel}$ with decreasing temperature.

II. SAMPLE PREPARATION AND CHARACTERIZATION

The samples were deposited by molecular beam epitaxy onto sapphire substrates with (110) orientation. Two electron beam sources were used for evaporating Nb and Ta in a preprogrammed sequence. In all cases, a 500-Å Ta layer was predeposited as a buffer and the final layers for all samples were Ta. During deposition, the pressure was kept below 10^{-8} Torr and the substrate temperature was held at 850 °C. The deposition rate was ~ 1 Å/sec. The quasiperiodic samples were constructed from Nb and Ta layers of thickness d_{Nb} and d_{Ta}, respectively, stacked according to a Fibonacci sequence as described previously by Merlin *et al.*[16] The ratio of these building block layers was chosen such that $d_{\mathrm{Nb}}/d_{\mathrm{Ta}} = \tau \equiv (1+\sqrt{5})/2$. The layer thicknesses of periodic specimens were chosen to provide approximately corresponding modulation wavelengths for comparison. In the following discussion we use the notation 55-34 when referring to the sample with $d_{\mathrm{Nb}} = 55$ Å and $d_{\mathrm{Ta}} = 34$ Å, etc. Table I lists the values of some of the relevant parameters for the samples studied.

All x-ray diffraction studies were carried out on four-circle diffractometers. High resolution (00l) scans (with the scattering vector normal to the sample plane) were performed with synchrotron radiation at the National Synchrotron Light Source at Brookhaven National Laboratory, and also with a rotating Mo-anode x-ray source fitted with a Ge monochromator and analyzer. In-plane scans were performed using the rotating Mo-anode source with a graphite monochromator. This results in lower instrumental resolution, but provides a high-intensity penetrating beam which is necessary in order to

TABLE I. Some relevant parameters for Nb-Ta superlattices. The first four samples have periodic layering, the latter four quasiperiodic (Fibonacci) layering.

Sample d_{Nb}(Å)/d_{Ta}(Å)	Thickness (Å)	R_R	l_0 (Å)	T_c (K)	$-dH_{c2\perp}/dT \mid_{T_c}$ (kG/K)	$-dH_{c2\parallel}/dT \mid_{T_c}$[a] (kG/K)
20-20	2000	3.36	80	6.06	2.37	3.46
80-80	1720	12.1	310	7.06	0.96	2.51
125-90	2500	10.7	260	7.52	0.97	1.74
180-110	5400	9.75	254	5.87	0.82	1.21
55-34	4180	5.04	85	7.97	1.69	2.56
100-62	2910	17.6	470	7.93	0.75	1.25
200-90	4360	9.51	225	8.23	0.99	1.82
225-139	6530	18.7	486	8.04	0.68	1.02

[a]Calculated from the linear portion of the curves at temperatures just below the negative curvature.

carry out these scans in transmission through the films without removing them from the substrates. The in-plane x-ray work will be reported in detail elsewhere,[18] while here we address the results which are relevant to the transport measurements.

In-plane ($hk0$) scans show that the samples are epitaxial single crystals growing in the (110) orientation on (110) sapphire, as found previously.[5–10] All of the samples, whether periodic or quasiperiodic, and regardless of layer thickness, show the same in-plane structure, i.e., all samples are single crystals with the same epitaxial relationship with respect to sapphire.

Out-of-plane c^* scans through the in-plane Nb-Ta (200) peak, such as that plotted in Fig. 1, clearly show superlattice satellites and a central peak about 0.01 Å^{-1} wide. These results indicate a high degree of stacking coherence between atomic planes and a crystal coherence length of $\pi/0.01 \approx 300$ Å.

Out of plane ($00l$) scans reveal the nature of the layering in the samples (either periodic or quasiperiodic) and the magnitudes of both interfacial diffusion and fluctuations in layer thicknesses. Layer thickness fluctuations (deviations from perfect periodic or Fibonacci superlattice ordering) arise from varying flux rates from the electron beam sources during growth, while interlayer diffusion is a consequence of the miscibility of Nb and Ta at these growth temperatures (850 °C).

In Fig. 2 we show a high-resolution out-of-plane scan for quasiperiodic sample 55-34. For all the quasiperiodic specimens it is possible to index 4 or 5 of the most intense satellites of the Nb-Ta (110) peak according to a scheme previously reported[16] for x-ray scattering from quasiperiodic samples. Here we do not attempt to index the large number of weaker peaks which arise from the quasi-

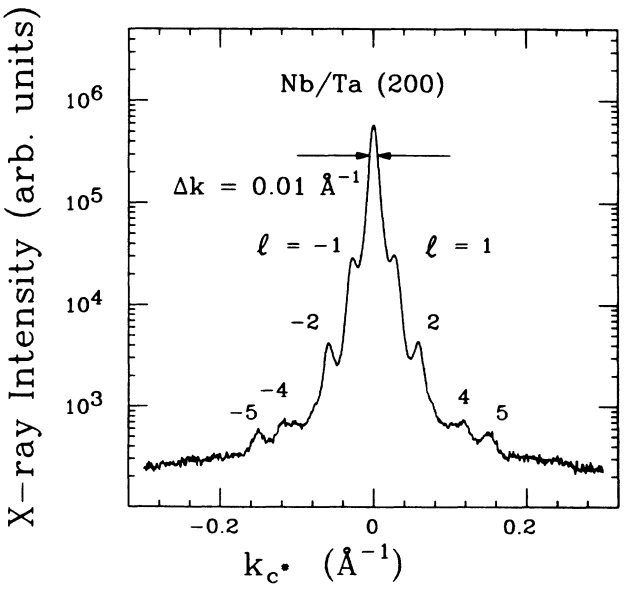

FIG. 1. ($20l$) x-ray scan through the in-plane (200) metal peak of periodic sample 125-90.

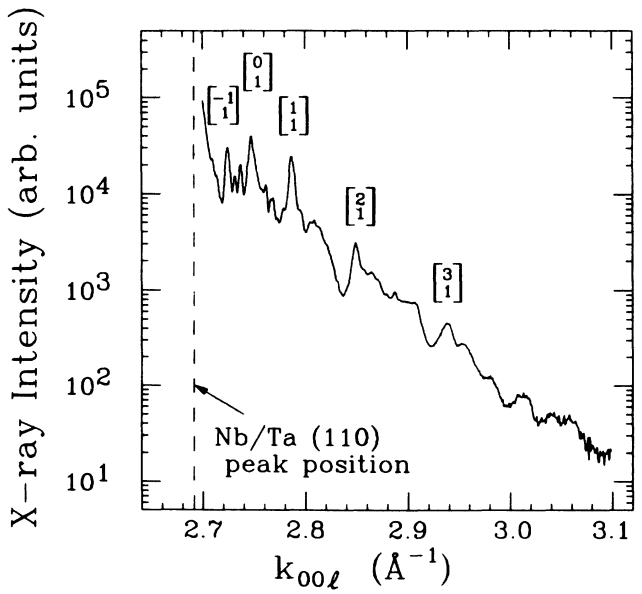

FIG. 2. High-resolution ($00l$) scan for quasiperiodic sample 55-34. The labels $[^m_n]$ correspond to an indexing scheme (Ref. 16) for quasiperiodic structures in which the diffraction vectors of the strongest peaks are $k - k_0 = (2\pi/d)n\tau^m$, where $k_0 = 2.691$ Å^{-1} denotes the position of the main (110) metal peak.

periodic ordering. Additional difficulty in indexing the peaks is associated with layering fluctuations and the limited number of Fibonacci building blocks present in these samples. These effects lead to attenuation, broadening, and a shift in position of the higher-order superlattice peaks. Nevertheless, the quasiperiodic and periodic samples can be distinguished by the nature of the prominent superlattice satellites, specifically by the appearance, in quasiperiodic specimens, of a series of satellites at positions occurring as powers of $\tau=(1+\sqrt{5})/2$ relative to the main metal peak.[16]

The magnitudes of interfacial diffusion and layer thickness fluctuations present in these samples have been estimated by matching the calculated scattering from a model unit cell (with fluctuations) to that measured experimentally. The results are presented in Fig. 3 for sample 20-20. In this model[18] we build a unit cell of 20 bilayers into which we incorporate (i) interlayer diffusion with an exponential profile (Fig. 3 inset) and (ii) variations in layer thickness with parabolic distributions about the means. We obtain a reasonably good fit with the data by using a diffusion layer thickness of approximately 9.5 Å (about four monolayers) and deposition rate fluctuations of 15%. For this 20-20 sample the rate fluctuations amount to layer thickness uncertainties of about one monolayer. The stacking coherence length of 300 Å calculated from the data for sample 125-90 (see Fig. 1) is typical of the larger modulation wavelength specimens and our estimates indicate that the magnitude of layer thickness fluctuations for these structures is no more than 5%. We compare the diffusion layer thickness to previous estimates of 4.5 Å at a growth temperature of 780 °C,[5] 6 Å at 600 °C,[8] 8 Å at 750 °C,[9] and 8.5 Å at 850 °C.[7] There are apparent discrepancies among these

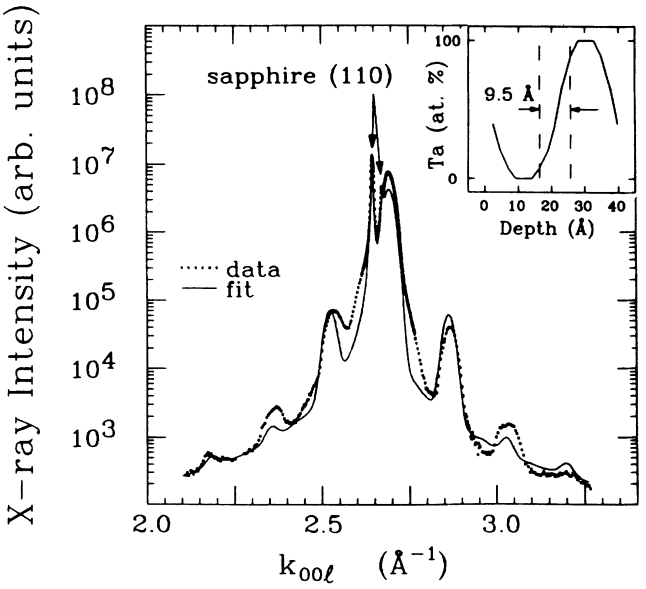

FIG. 3. (00l) scan for periodic sample 20-20. The solid line is a fit to a model incorporating both interdiffusion at the interfaces and layer thickness fluctuations. The inset shows the composition profile from the model fitting parameters.

data which may be accounted for by differences among the various studies in the interpretation of the x-ray data, accurate substrate temperature measurement during growth, total growth times, and interfacial compositional roughness or terracing that may mimic interdiffusion. Interfacial terrace formation may be related to vacuum conditions during growth, with lower background pressures favoring the formation of smoother interfacial surfaces.

For transport measurements, the samples were patterned by cutting a bridge 15-mm long and 1-mm wide with a diamond saw mounted on a manipulator. Standard four-probe electrical contacts were made with silver epoxy to the topmost layer of the specimens. Measurements were carried out in a conventional ^{4}He cryostat equipped with a 6-T split-coil superconducting magnet. Mounted on a rotating platform, this magnet provided fields in any orientation with respect to the layer planes to an accuracy of $\pm 1/2°$. dc measurements were performed with a current density of 5–15 A/cm^2. The upper critical-field curves were determined at fixed magnetic field increments by adjusting temperature through the transition with $T_c(H)$ defined by the 50% resistive transition. Temperature was determined by a calibrated carbon glass sensor.

The parallel resistance ratios, $R_R \equiv \rho(300\ \mathrm{K})/\rho(10\ \mathrm{K})$, and critical temperatures, T_c, for our samples are listed in Table I. Using a value[9] of $\rho l = 370\ \mu\Omega\,\mathrm{cm}\ \text{Å}$, we have also calculated low-temperature mean free paths, l_0. These values are a factor of 2–3 larger than $d_{\mathrm{Nb,Ta}}$ for all samples, reflecting the relatively high quality of the interfaces in these superlattices. As expected for proximity coupled systems, the critical temperatures are reduced from the bulk Nb value of 9.3 K due to the proximity of the lower-T_c Ta layers ($T_c^{\mathrm{bulk}}=4.4$ K). The T_c's of the quasiperiodic samples are consistently higher than those with periodic layering, presumably due to the larger Nb fraction of the former. The critical temperature of sample 180-110 is, however, surprisingly low. The relatively high R_R of this specimen, 9.75, indicates that it is moderately clean in a superconducting sense [the dirty limit applies for $l_0 \ll \xi_0$ where ξ_0 is the Bardeen-Cooper-Schrieffer (BCS) coherence length]. In spite of this, the transition temperature is below the Cooper limit[19] estimate of ~ 6.6 K, valid for thin ($\xi_0 \gg d_{N,S}$) bilayers in the dirty limit. Indeed, the T_c for 180-110 is even below that of 20-20 which has a substantially lower R_R. While we expect alloy formation in the interfacial regions to be particularly important for 20-20, clearly this is not as important for 180-110. An equally low T_c was found by Durbin[6] for a Nb-Ta superlattice ($\Lambda=85$ Å, $R_R=4.6$), and was attributed to oxygen impurities. Interstitial oxygen increases resistivity[20] and reduces T_c (Ref. 21) in bulk Nb at rates of 5.0 $\mu\Omega$ cm/at. % and 0.9 K/at. %, respectively. Though these rates have not been established for thin films and multilayers, oxygen impurities could possibly account for the lower T_c of these specimens. We note, however, that oxygen would also tend to enhance H_{c2},[21] yet the upper critical fields for 180-110 appear consistent with those of the other samples in the series. We have also measured superconducting transition widths, defined

by the 10–90% transition points. The zero-field values range from 39 to 73 mK for periodic samples and are a factor of 2–5 larger for quasiperiodic specimens. The widths for both types of samples have an anomalous magnetic field dependence in both perpendicular and parallel orientations, and will be discussed in detail elsewhere.[22]

III. UPPER CRITICAL FIELDS

Perpendicular upper critical fields for several periodic and quasiperiodic samples are plotted in reduced units in Fig. 4. Sample 20-20 with the thinnest layers exhibits the typical $h \propto 1-t$ behavior expected for bulk, homogeneous superconductors. The other samples show a positive curvature below $t \sim 0.85$ that becomes more pronounced with increasing layer thickness. A similar trend was reported recently[9] for periodic Nb-Ta multilayers with larger modulation wavelengths. There it was suggested that positive curvature is associated with clean Nb layers and their characteristic Fermi surface anisotropy, thus appearing enhanced for specimens with larger Nb layer thickness. That this effect is more marked in quasiperiodic samples 225-139 and 200-90 might be a consequence of the presence of Nb layers of thickness $2d_{\mathrm{Nb}}$ (as well as d_{Nb}) along the Fibonacci chain, thus giving these specimens effectively cleaner Nb layers. With this interpretation the data of Fig. 4 tend to support the results of Ref. 9.

Parallel critical fields for periodic and quasiperiodic samples are shown in Figs. 5(a) and 5(b), respectively. Evident in these data are negative curvature near $t=1$, and upturns (marked by arrows) which are similar in character to those typically associated with three-dimensional to two-dimensional (3D→2D) transitions. From anisotropic Ginzburg-Landau theory,[23] the upper critical fields are expressed in terms of the parallel and perpendicular coherence lengths by

$$H_{c2\parallel}(T)=\frac{\phi_0}{2\pi\xi_\parallel(T)\xi_\perp(T)}\ ,$$
$$H_{c2\perp}(T)=\frac{\phi_0}{2\pi\xi_\parallel^2(T)}\ , \tag{1}$$

where ϕ_0 is the flux quantum. In general, for an S-N system one anticipates a 3D→2D transition for $\xi_\perp > d_S$ when $\xi_\perp$ goes from $\gg d_N$, where the S layers are strongly coupled, to $\ll d_N$, where they behave independently. Except for the negative curvature near T_c, which we address below, the thin-layered specimens exhibit the $H_{c2} \propto (1-t)$ behavior expected for bulk superconductors. The upturn evident for specimen 180-110 occurs at $t \sim 0.6$ where we estimate $\xi_\perp \sim 290$ Å using (1). Apparently a dimensional crossover has taken place with $H_{c2\parallel}$ displaying the $(1-t)^{1/2}$ dependence characteristic of 2D superconductivity for $t < 0.6$. In periodic superconductor-insulator(S-I) systems[24] dimensional crossover occurs when $\xi_\perp/\Lambda=\sqrt{2}$, where $\Lambda=d_S+d_I$, however for metallic multilayers there is no well-defined criterion for dimensional crossover. The order parameter

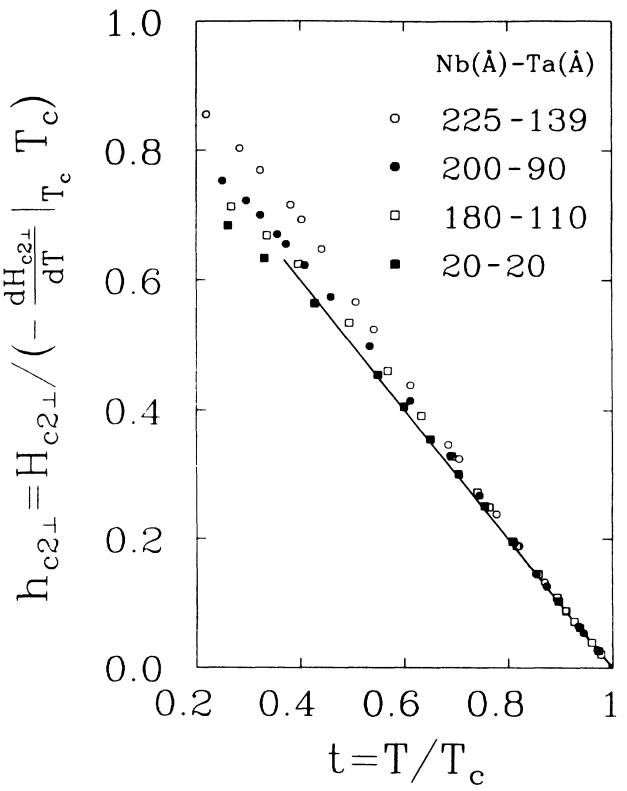

FIG. 4. Perpendicular upper critical field vs temperature, plotted in reduced units for several periodic and quasiperiodic samples. The straight line is drawn proportional to $(1-t)$.

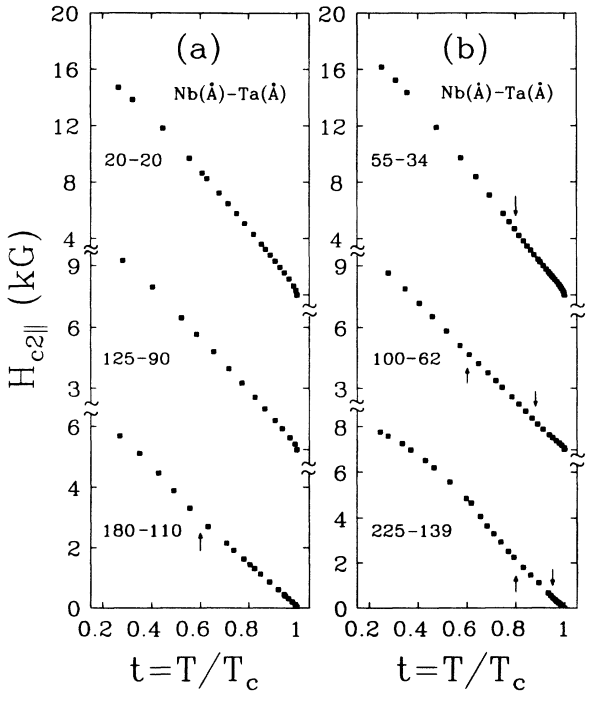

FIG. 5. Parallel upper critical field vs reduced temperature for samples with (a) periodic and (b) quasiperiodic layering. Arrows indicate upturns as discussed in text.

in a proximity-coupled system will tend to nucleate in the S layers and may extend into the adjacent N layers. The range of this penetration will depend, in principle, on the electronic diffusion constant in the N layers and on the properties of the interfacial regions. A reasonable criterion for a transition to a 2D-like behavior would seem to be $\xi_\perp \leq d_S + d_N$, allowing for penetration a distance $d_N/2$ into the adjacent N layers. The value of $\xi_\perp$ at the upturn in 180-110 supports this picture. Dimensional crossover should also be evident in the angular dependence of the upper critical field, $H_{c2}(\theta)$. For an anisotropic 3D superconductor, the angular dependence is given by

$$H_{c2}(T,\theta) = \frac{H_{c2\perp}(T)}{[(m/M)\sin^2\theta + \cos^2\theta]^{1/2}} , \tag{2}$$

where

$$M/m = \left[\frac{H_{c2\parallel}(T)}{H_{c2\perp}(T)} \right]^2 .$$

For a 2D film ($\xi > d$), $H_{c2}(\theta)$ satisfies the equation[25]

$$\left| \frac{H_{c2}(T,\theta)\cos\theta}{H_{c2\perp}(T)} \right| + \left[\frac{H_{c2}(T,\theta)\sin\theta}{H_{c2\parallel}(T)} \right]^2 = 1 . \tag{3}$$

These angular dependences are qualitatively distinguished at parallel field ($\theta = 90°$), where the peak is either rounded (3D) or cusplike (2D). Figure 6 shows $H_{c2}(\theta)$ at several temperatures for sample 180-110. At $t \sim 0.88$, well above the crossover temperature, the data show a cusp in parallel field that fits well with the 2D Eq. (3). At this temperature, $\xi_\perp \sim 500$ Å, and though we do not expect 2D behavior, apparently the order parameter does not extend over sufficiently many layers to yield averaged, anisotropic 3D behavior. In the limit of small layer thickness we do observe the dependence predicted by Eq. (2), with zero slope, $dH_{c2}(\theta)/dT$, at parallel field (shown for 55-34 in Fig. 7). With decreasing temperature, $H_{c2}(\theta)$ for 180-110 becomes very sharply peaked at parallel field, and cannot be fitted to a 2D or surface state angular dependence. A similar angular dependence was reported in Ref. 9 for $\xi_\perp < d_{Nb}$. Apparently the sharpening of the peak in parallel field occurs as superconductivity becomes increasingly localized in the Nb layers.

No upturns are evident in $H_{c2\parallel}$ for the other periodic specimens, and this is generally expected for shorter modulation wavelengths where thinner layers are more strongly coupled. The apparent lack of such a feature in the data for sample 125-90 is somewhat surprising in view of the fact that we do observe upturns in quasiperiodic samples 55-34 and 100-62 which have comparable or smaller layer thicknesses. We now discuss those results.

The $H_{c2\parallel}$ curves for quasiperiodic specimens 100-62 and 225-139 exhibit two upturns with decreasing temperature [Fig. 5(b)]. The higher temperature upturns are clearly visible in Fig. 8 where we have expanded the region near T_c. As mentioned above, these samples are characterized by two fundamental Nb length scales, d_{Nb} and $2d_{Nb}$. We attribute the higher(lower) temperature

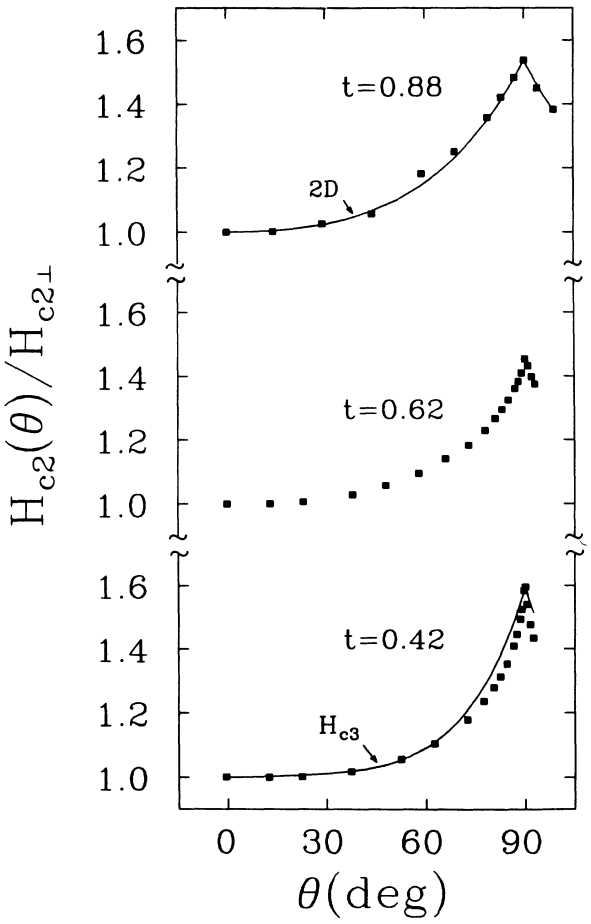

FIG. 6. $H_{c2}(\theta)/H_{c2\perp}$ vs θ for sample 180-110 at several temperatures. Note the sharpening of the peak at parallel field that occurs below the upturn temperature ($t = 0.6$) for $H_{c2\parallel}$ [Fig. 5(a)]. The solid lines are fits to ($t = 0.88$) the 2D equation (3) and ($t = 0.42$) the surface state dependence.

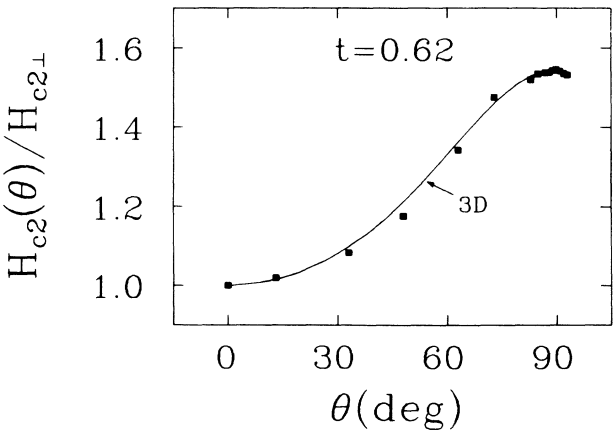

FIG. 7. $H_{c2}(\theta)/H_{c2\perp}$ vs θ for sample 55-34 at $t = 0.62$. The solid line is a fit to the 3D theory, Eq. (2).

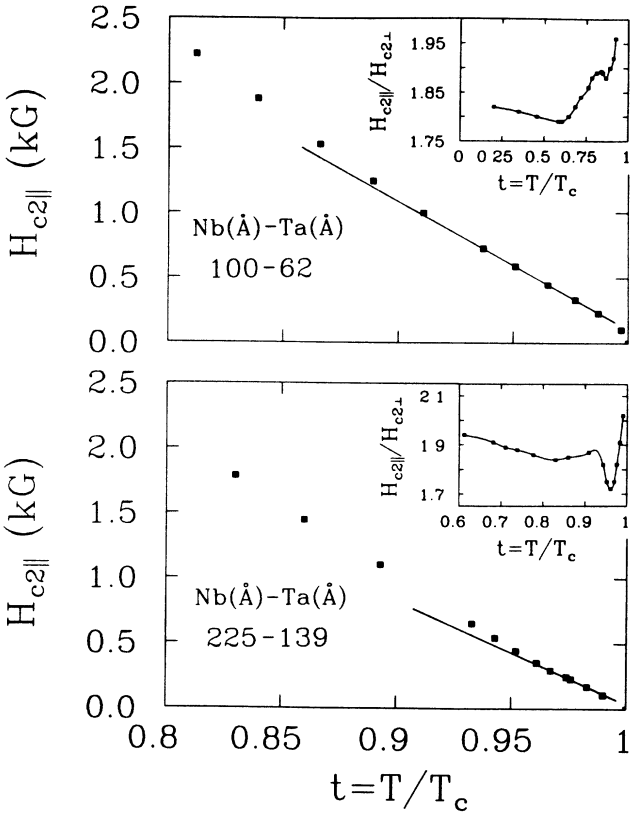

FIG. 8. Expanded portion of $H_{c2\|}$ vs t curves [Fig. 5(b)] for quasiperiodic samples 100-62 and 225-139 showing the high temperature upturns. The insets show the anisotropy ratios, $H_{c2\|}/H_{c2\perp}$, plotted vs reduced temperature for each sample. Solid lines are guides to the eye.

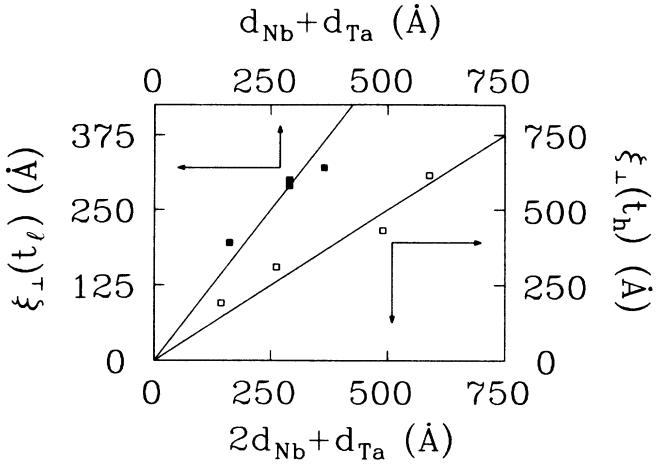

FIG. 9. $\xi_\perp(t_h)$ vs $2d_{Nb}+d_{Ta}$ (lower and right scales) and $\xi_\perp(t_l)$ vs $d_{Nb}+d_{Ta}$ (upper and left scales) for the samples listed in Table II. The solid lines are $\xi_\perp(t_h)=2d_{Nb}+d_{Ta}$ and $\xi_\perp(t_l)=d_{Nb}+d_{Ta}$.

upturns to dimensional crossover associated with the Nb layers of thickness $2d_{Nb}(d_{Nb})$. Dimensional crossover will, in general, result in an increase in the anisotropy ratio, $H_{c2\|}/H_{c2\perp}$, and this quantity is plotted as a function of temperature for these specimens in the insets of Fig. 8. Guided by the results for 180-110 the high- and low-temperature transitions (denoted t_h and t_l) would be expected for $\xi_\perp(t_h)\leq 2d_{Nb}+d_{Ta}$ and $\xi_\perp(t_l)\leq d_{Nb}+d_{Ta}$, respectively. The values of these dimensional crossover parameters are summarized in Table II for all samples showing upturns in $H_{c2\|}$ or, equivalently, in $H_{c2\|}/H_{c2\perp}$. The agreement between $\xi_\perp$ and the expected values is quite good as shown graphically in Fig. 9. The poorest agreement is found for the upturn in sample 55-34, and may be associated with the interfacial regions which represent a substantial fraction of the layer thicknesses in this specimen. We note that the high-t and low-t upturns observed by Broussard and Geballe[9] are apparently[26] associated with transitions to 2D-like behavior in the Ta and Nb layers, respectively, representing the new phase diagram predicted by Takahashi and Tachiki.[2] The 2D-like Ta transition is not favored in our samples because of the relatively thin Ta layers employed. The thin Ta layers are probably also the reason why the upturns for these samples are less dramatic than those associated with previously reported 3D→2D transitions. It should be emphasized that the double crossover behavior observed here does not appear to be a consequence of the aperiodicity (i.e., Fibonacci sequence) *per se*, and should appear in periodic *S-N* or *S-I* multilayers having two different *S*-layer thicknesses of appropriate size relative to $\xi_\perp$.

Finally, we address the negative curvature in $H_{c2\|}$ near T_c. This behavior is clearly not a consequence of the nature of the layering as it appears in all specimens regardless of layering sequence. The curvature extends to lower temperatures and higher fields in specimens with thinner layers, suggesting that the multilayering is important. We note that the superconducting resistive transitions in the curvature region exhibit a plateau as a function of

TABLE II. Values of characteristic dimensional crossover parameters.

Sample d_{Nb}(Å)/dTa(Å)	t_h	t_l	$\xi_\perp(t_h)$ (Å)	$\xi_\perp(t_l)$ (Å)	$2d_{Nb}+d_{Ta}$ (Å)	$d_{Nb}+d_{Ta}$ (Å)
55-34	0.80		190		144	89
100-62	0.86	0.60	310	195	262	162
180-110		0.60		290		290
200-90	0.93	0.87	430	300	490	290
225-139	0.95	0.83	615	320	589	364

temperature. The origin of this behavior is not clear and will be pursued in a discussion of transition widths.[22]

In summary, we have investigated the superconducting properties of periodic and quasiperiodic Nb-Ta multilayers. In agreement with a previous study,[9] the positive curvature in $H_{c2\perp}$ observed for both types of layering would seem to be associated with clean Nb, appearing more pronounced for specimens composed of thicker Nb layers. Negative curvature near T_c in $H_{c2\parallel}$ does not appear to be related to the nature of layering. Dimensional crossover occurs for both types of layering when $\xi_\perp$ becomes comparable to the modulation wavelength. In quasiperiodic specimens two crossovers are observed with decreasing temperature, arising as $\xi_\perp$ probes the two length scales, $2d_{\mathrm{Nb}}$ and d_{Nb}, present in these structures.

ACKNOWLEDGMENTS

This work was supported by National Science Foundation Materials Research Group Grant No. DMR-8602675. One of us (F.J.L.) was supported, in part, by the Army Research Office under Grant No. DAAL-03-86-G-0053. It is a pleasure to thank Roberto Merlin for useful discussions and to acknowledge the help of J. D. Axe, K. M. Mohanty, and B. Rodricks at the X22B beamline of the National Synchrotron Light Source, Brookhaven National Laboratory. This portion of the work was carried out under the U.S. Department of Energy Contract No. DE-AC02-76CH00016. One of us (C.U.) acknowledges additional support from the University of Michigan Phoenix Memorial Grant.

*Present address: Department of Physics, University of Virginia, Charlottesville, VA 22901.

[1]S. Takahashi and M. Tachiki, Phys. Rev. B **33**, 4620 (1986).

[2]S. Takahashi and M. Tachiki, Phys. Rev. B **34**, 3612 (1986).

[3]K. R. Biagi, V. G. Kogan, and J. R. Clem, Phys. Rev. B **32**, 7615 (1985).

[4]Madhu Menon and Gerald B. Arnold, Superlatt. Microstr. **1**, 451 (1985).

[5]S. M. Durbin, J. E. Cunningham, M. E. Mochel, and C. P. Flynn, J. Phys. F **11**, L223 (1981); S. M. Durbin, J. E. Cunningham, and C. P. Flynn, *ibid.* **12**, L75 (1982).

[6]S. M. Durbin, Ph.D. thesis, University of Illinois at Urbana-Champaign, 1983.

[7]G. Hertel, D. B. McWhan, and J. M. Rowell, in *Proceedings of the IV Conference on Superconductivity in d- and f-band Metals* (Kernforschugszentrum, Karlsruhe, 1982), p. 299.

[8]Y. Nishihata, M. Nakayama, H. Kato, N. Sano, and H. Terauchi, J. Appl. Phys. **60**, 3523 (1986).

[9]P. R. Broussard and T. H. Geballe, Phys. Rev. B **35**, 1664 (1987).

[10]C. Uher, J. L. Cohn, P. Miceli, and H. Zabel, Phys. Rev. B **36**, 815 (1987).

[11]I. Banerjee, Q. S. Yang, C. M. Falco, and I. K. Schuller, Phys. Rev. B **28**, 5037 (1983).

[12]C. S. L. Chun, G. G. Zheng, J. L. Vicent, and I. K. Schuller, Phys. Rev. B **29**, 4915 (1984).

[13]K. Kanoda, H. Mazaki, T. Yamada, N. Hosoito, and T. Shinjo, Phys. Rev. B **33**, 2052 (1986); K. Kanoda, H. Mazaki, N. Hosoito, and T. Shinjo, *ibid.* **35**, 6736 (1987).

[14]M. G. Karkut, J. M. Triscone, D. Ariosa, and O. Fischer, Phys. Rev. B **34**, 4390 (1986).

[15]For a review, see, e.g., *Synthetic Modulated Structures,* edited by L. Chang and B. C. Giessen (Academic, New York, 1984).

[16]R. Merlin, K. Bajema, R. Clarke, F. Y. Juang, and P. K. Bhattacharya, Phys. Rev. Lett. **55**, 1768 (1985).

[17]V. Matijasevic and M. R. Beasley, Phys. Rev. B **35**, 3175 (1987).

[18]R. Clarke, F. Lamelas, and H. He (unpublished).

[19]L. N. Cooper, Phys. Rev. Lett. **6**, 689 (1961).

[20]T. Ohtsuka and Y. Kimura, Physica **55**, 562 (1971).

[21]C. C. Koch, J. O. Scarbrough, and D. M. Kroeger, Phys. Rev. B **9**, 888 (1974).

[22]J. L. Cohn, J. J. Lin, and C. Uher (unpublished).

[23]W. E. Lawrence and S. Doniach, in *Proceedings of the 12th International Conference on Low Temperature Physics, Kyoto,* edited by E. Kanda (Academic, Tokyo, 1971), p. 361.

[24]R. A. Klemm, M. R. Beasley, and A. Luther, J. Low Temp. Phys. **16**, 607 (1974).

[25]M. Tinkham, Phys. Rev. **129**, 2413 (1963).

[26]P. R. Broussard, Ph.D. thesis, Stanford University, 1986.